



a **P**ayload for **A**ntimatter **M**atter **E**xploration
and **L**ight-nuclei **A**strophysics

Observations of solar particle events with the PAMELA mission

A. Bruno*, G.C. Bazilevskaya, M. Boezio, E.R. Christian, G.A. de Nolfo,
V. Di Felice, M. Martucci, M. Mergé, V.V. Mikhailov, R. Munini, J.M. Ryan, S. Stochaj

*INFN, Sezione di Bari, Italy



on behalf of the PAMELA collaboration



Solar Energetic Particles (SEP), Solar Modulation and
Space Radiation: New Opportunities in the AMS-02 Era #2
Washington DC, 24-26 April 2017

The PAMELA collaboration

Payload for Antimatter Matter Exploration and Light-nuclei Astrophysics

Italy:



Bari



Florence



Frascati



Naples



Tor Vergata
Rome



Trieste

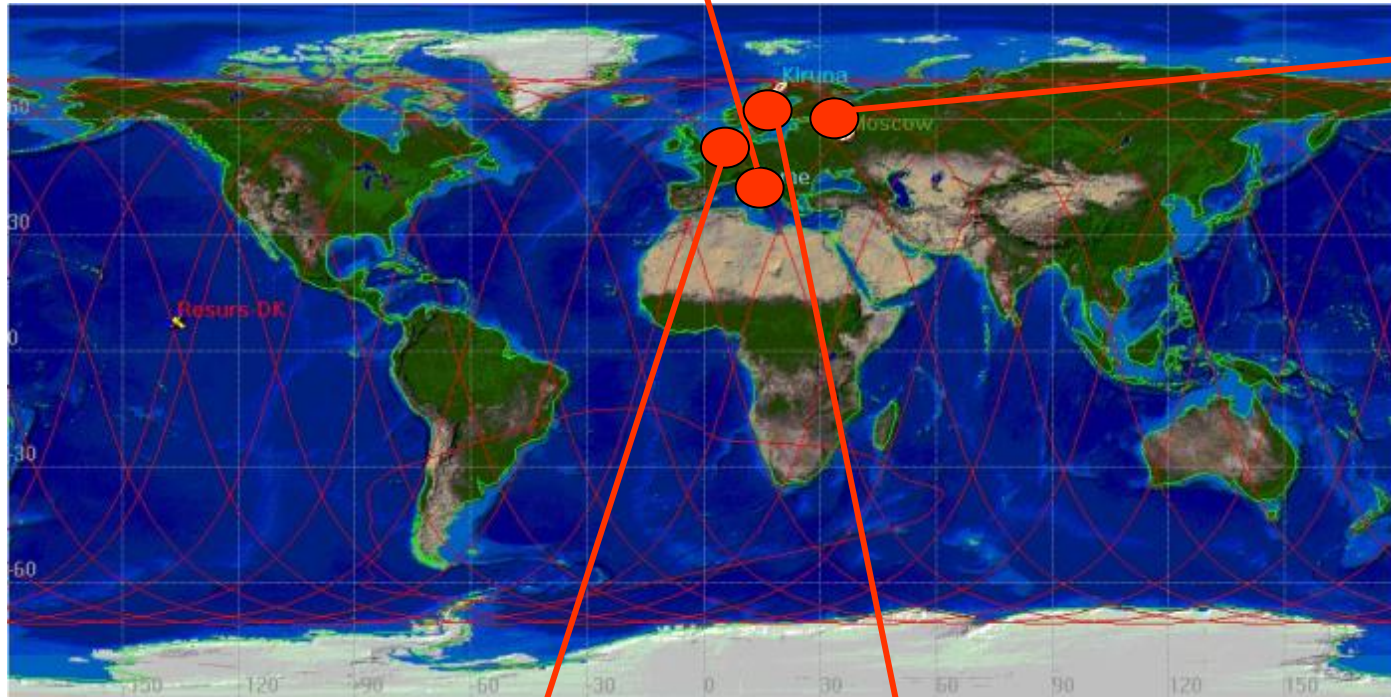


CNR, Florence

Russia:



Moscow
St. Petersburg



Germany:



Siegen

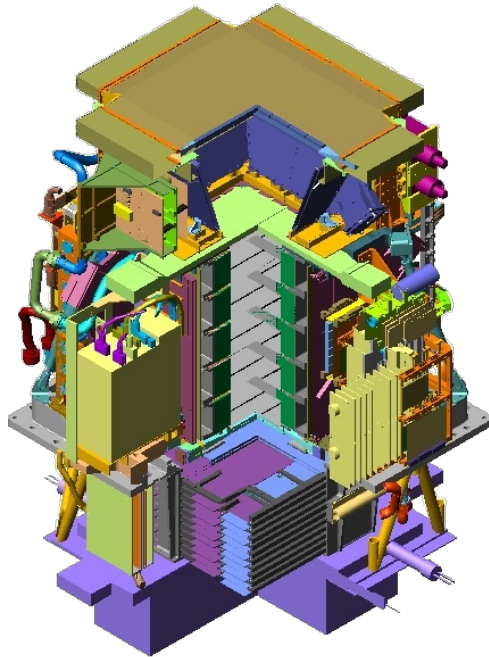
Sweden:



KTH, Stockholm

The PAMELA experiment

Main requirements → high-sensitivity particle identification and precise momentum measure



Size: 130x70x70 cm³
GF: 21.5 cm² sr
Mass: 470 kg
Power Budget: 360W

Resurs DK-1 satellite:

Semi-polar (70° inclination)
and elliptical (350÷610 km
altitude) orbit

Time-Of-Flight

plastic scintillators + PMT

- Trigger
- Albedo rejection;
- Mass identification up to 1 GeV;
- Charge identification from dE/dX .

Anticoincidence shield

plastic scintillators + PMT

Electromagnetic calorimeter

W/Si sampling (16.3 X_0 , 0.6 λ)

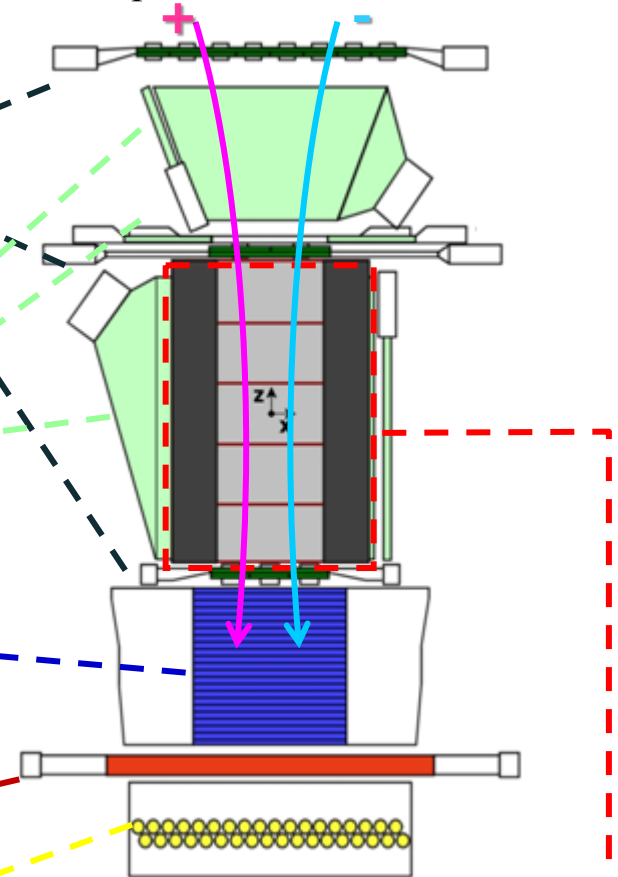
- Discrimination e^+ / p, anti-p / e^-
(shower topology)
- Direct E measurement for e^-

Bottom scintillator (+PMT)

Neutron detector

³He counters

- High-energy e/h discrimination



Spectrometer

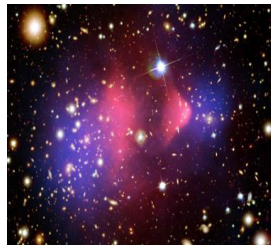
microstrip silicon tracking system
+ permanent magnet

- Magnetic rigidity: $R=pc/Ze$
- Charge sign
- Charge value from dE/dx
- Particle direction

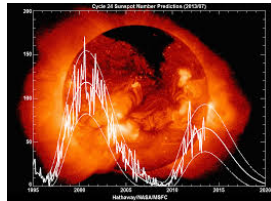
PAMELA scientific goals



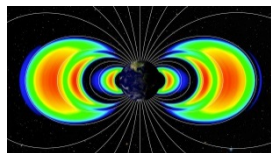
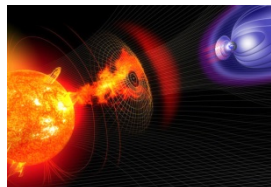
Precise measurements of protons, electrons, their antiparticles and light nuclei in the cosmic radiation



- Research for Dark Matter indirect signatures
- Exploration of the particle/antiparticle symmetry



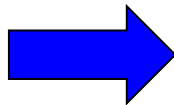
- Investigation of the cosmic-ray origin and propagation mechanisms in the Galaxy, the heliosphere and the terrestrial magnetosphere



- detailed measurement of the high energy particle populations (galactic, solar, geomagnetically trapped and albedo) in the near-Earth radiation environment

SEP measurements with PAMELA

- ❖ wide energy interval (above ~ 80 MeV)
 - bridging the low energy data by other space-based instruments and the GLE data by the worldwide network of neutron monitors (NMs)
- ❖ sensitive to particle composition
 - protons, He nuclei, ...
- ❖ possibility to reconstruct the angular (or pitch-angle) distribution
 - investigation of flux anisotropies



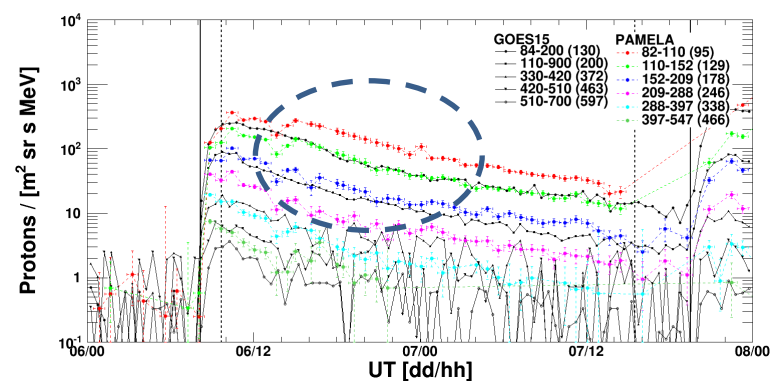
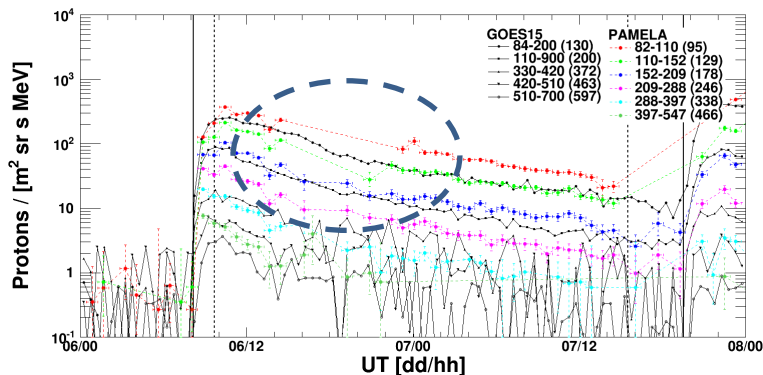
complete view of SEP events !

Flux reconstruction

- Thanks to the 70 deg inclination orbit, PAMELA can sample interplanetary particles down to the lowest cutoff rigidities (magnetic polar regions)
- To discard trapped and albedo particles and avoid magnetospheric effects, interplanetary CR fluxes are conservatively estimated by selecting protons with rigidity 1.3 times higher than the local vertical Störmer cutoff.
- The duty cycle increases with proton energy due to geomagnetic cutoff effects along the orbit
- Differential fluxes are evaluated on a relatively short time scale (48 min) corresponding to spacecraft semi-orbits

Flux reconstruction

- The background associated to galactic CR protons is evaluated by averaging the fluxes measured by PAMELA during periods of quiet solar conditions, within ~ 2 Carrington rotation intervals around each SEP event.
- Pitch angle anisotropies with respect to the local IMF direction (onset phase) are properly estimated by accounting for the instrument asymptotic exposition along the satellite orbit (back-tracing techniques)
- Event-integrated fluences are corrected for missing orbits by means of interpolation methods:



List of PAMELA events (2006-2014)

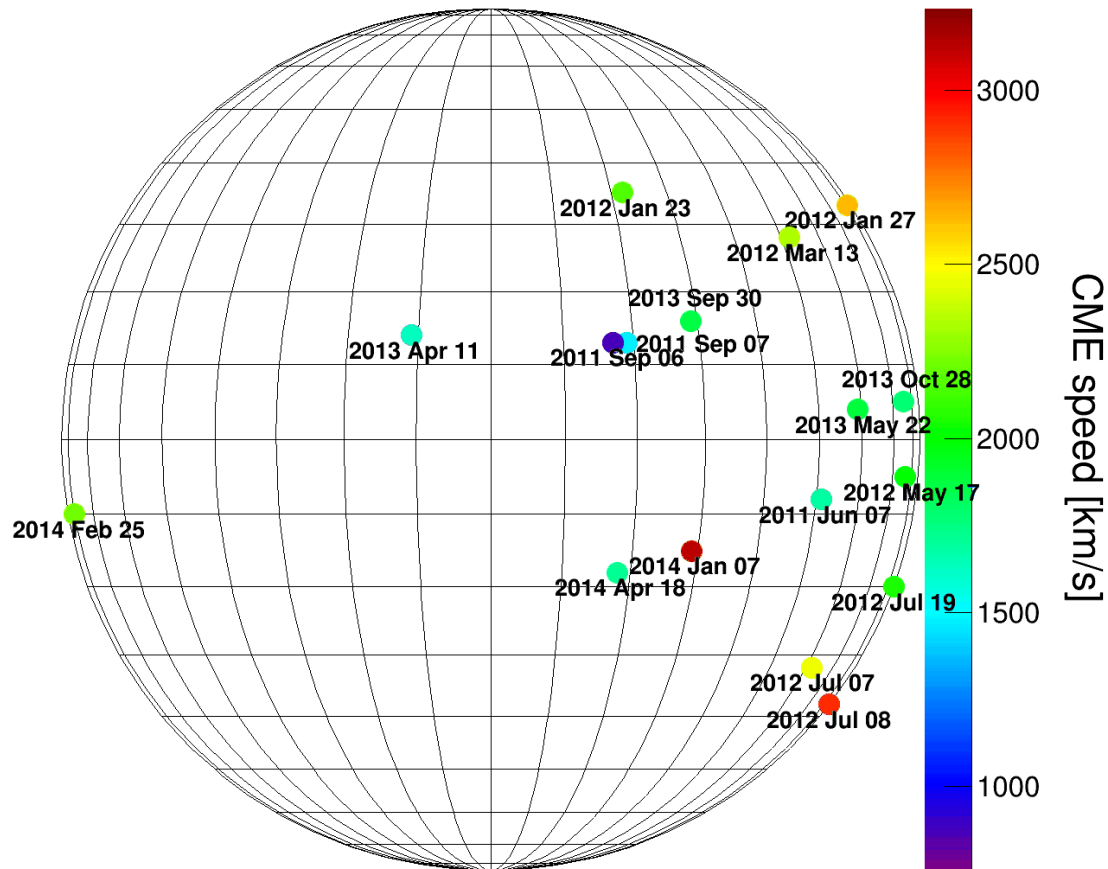
| Event No. | Date | Class | Location |
|-----------|-------------|---------|----------|
| 1 | 2006 Dec 13 | X3.4/4B | S06W23 |
| 2 | 2006 Dec 14 | X1.5/-- | S06W46 |
| 3 | 2011 Mar 21 | M3.7/-- | >W90 |
| 4 | 2011 Jun 07 | M2.5/2N | S21W54 |
| 5 | 2011 Sep 06 | M5.3/-- | N14W07 |
| 6 | 2011 Sep 07 | X2.1/-- | N14W18 |
| 7 | 2011 Nov 04 | ? | ? |
| 8 | 2012 Jan 23 | M8.7/-- | N28W21 |
| 9 | 2012 Jan 27 | X1.7/1F | N27W71 |
| 10 | 2012 Mar 07 | X5.4/- | N17E27 |
| 11 | 2012 Mar 13 | M7.9/-- | N17W66 |
| 12 | 2012 May 17 | M5.1/1F | N11W76 |
| 13 | 2012 Jul 07 | X1.1/-- | S13W59 |
| 14 | 2012 Jul 08 | M6.9/1N | S17W74 |

| Event No. | Date | Class | Location |
|-----------|-------------|---------|----------|
| 15 | 2012 Jul 19 | M7.7/-- | S13W88 |
| 16 | 2012 Jul 23 | ? | >W90 |
| 17 | 2013 Apr 11 | M6.5/3B | N09E12 |
| 18 | 2013 May 22 | M5.0/-- | N13W75 |
| 19 | 2013 Sep 30 | C1.3/-- | N17W29 |
| 20 | 2013 Oct 28 | M5.1 | N08W71 |
| 21 | 2013 Nov 02 | ? | ? |
| 22 | 2014 Jan 06 | ? | >W90 |
| 23 | 2014 Jan 07 | X1.2/-- | S15W11 |
| 24 | 2014 Feb 25 | X4.9/B | S12E82 |
| 25 | 2014 Apr 18 | M7.3/-- | S20W34 |
| 26 | 2014 Sep 01 | ? | >W90 |
| 27 | 2014 Sep 10 | X1.6/-- | N14E02 |

All flares are associated with (halo) CMEs

Red=back-side events; blue=eastern limb events

Heliographic map of PAMELA events



CME data are from **Gopalswamy et al. (2014, 2015)**.

Initial source locations are corrected for the solar B0 angle and the non-radial CME motion.

The *sky-plane* speeds are from the SOHO/LASCO catalog. *Peak space* speeds attained by the CMEs (used in this work) are derived from the flux-rope fit.

The Ellison-Ramaty fit

$$F(E) = A \times \left(\frac{E}{80} \right)^{-\gamma} \times \exp\left(-\frac{E}{E_c} \right)$$

normalization

spectral index

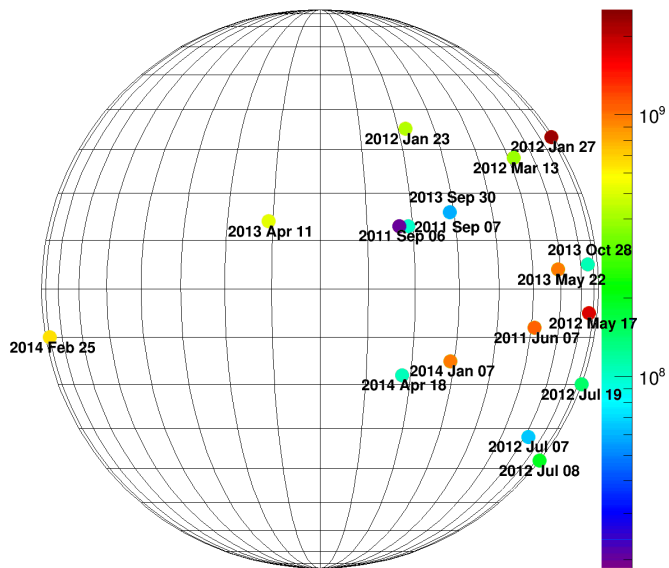
scaling energy
(fixed, =PAMELA threshold)

roll-over or
cutoff energy

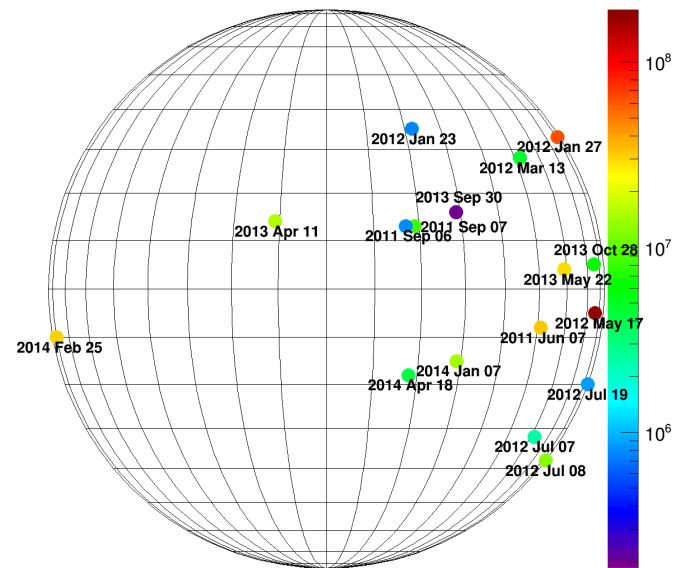
Roughly speaking, the slope of the power law is related to the Mach number and the compression ratio, which govern the efficiency for shock acceleration, while the cutoff energy is a reflection of the loss mechanisms (e.g., available acceleration time). The «scaling» energy is useful to decorrelate A and γ .

Event-integrated fluences vs heliographic locations

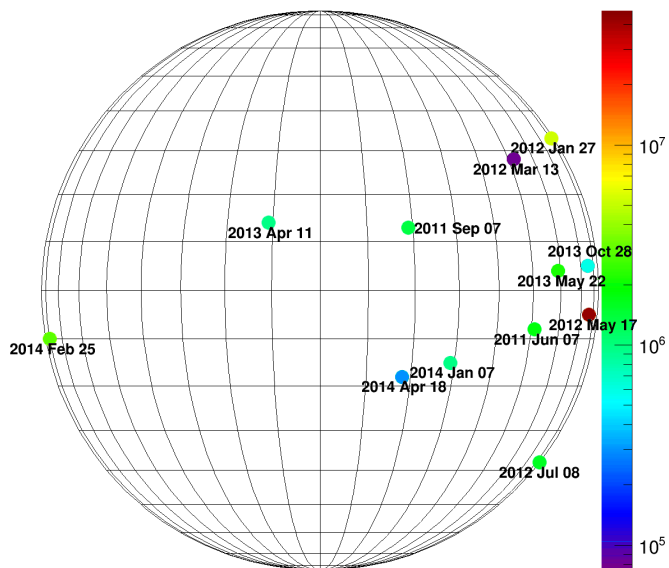
Event-integrated fluences ($E > 100$ MeV) [$\text{sr}^{-1}\text{m}^{-2}$]



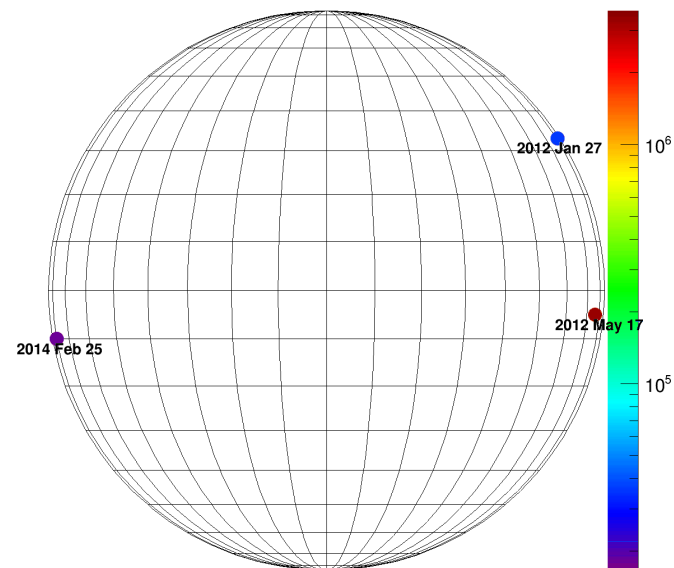
Event-integrated fluences ($E > 300$ MeV) [$\text{sr}^{-1}\text{m}^{-2}$]



Event-integrated fluences ($E > 500$ MeV) [$\text{sr}^{-1}\text{m}^{-2}$]



Event-integrated fluences ($E > 1000$ MeV) [$\text{sr}^{-1}\text{m}^{-2}$]



Correlation studies

Flares

- X-ray peak flux
- fluence
- rise time
- duration
- location

CMEs

- speed
- kinetic energy
- mass
- location/direction

SEPs

- event-integrated fluences
- peak fluxes (to be done)
- E-R fit parameters
- Duration
- Delay/propagation time (to be done)

Investigation of (semi-)empirical statistical relations between the observed properties (deductive approach)

SEP correlations

preliminary!

| | X-ray peak flux | X-ray duration | X-ray rise time | CME speed | CME kinetic energy | CME mass | Latitude total / <22deg only | Longitude |
|----------|-----------------|----------------|-----------------|-----------|--------------------|----------|------------------------------|-----------|
| A | 0.07 | 0.62 | 0.33 | 0.42 | 0.86 | 0.74 | 0.04/-0.24 | 0.05 |
| γ | 0.00 | 0.16 | 0.42 | 0.44 | 0.63 | 0.45 | -0.07/0.25 | 0.17 |
| E_c | 0.03 | 0.04 | 0.00 | 0.16 | 0.30 | 0.40 | -0.34/-0.47 | 0.20 |
| F>80 | 0.09 | 0.57 | 0.31 | 0.37 | 0.83 | 0.80 | -0.06/-0.50 | 0.08 |
| F>100 | 0.10 | 0.56 | 0.30 | 0.32 | 0.77 | 0.79 | -0.14/-0.57 | 0.11 |
| F>300 | -0.03 | 0.34 | 0.36 | 0.09 | 0.38 | 0.58 | -0.37/-0.53 | 0.18 |
| F>500 | -0.14 | 0.24 | 0.40 | -0.02 | 0.19 | 0.49 | -0.32/-0.43 | 0.32 |
| F>700 | -0.21 | 0.26 | 0.39 | -0.10 | 0.14 | 0.44 | -0.36/-0.44 | 0.31 |

Correlation coefficients for the E-R fit parameters (A, γ , E_c) and the event-integrated fluences at different thresholds (>80, >100, >300, >500, >700 MeV)

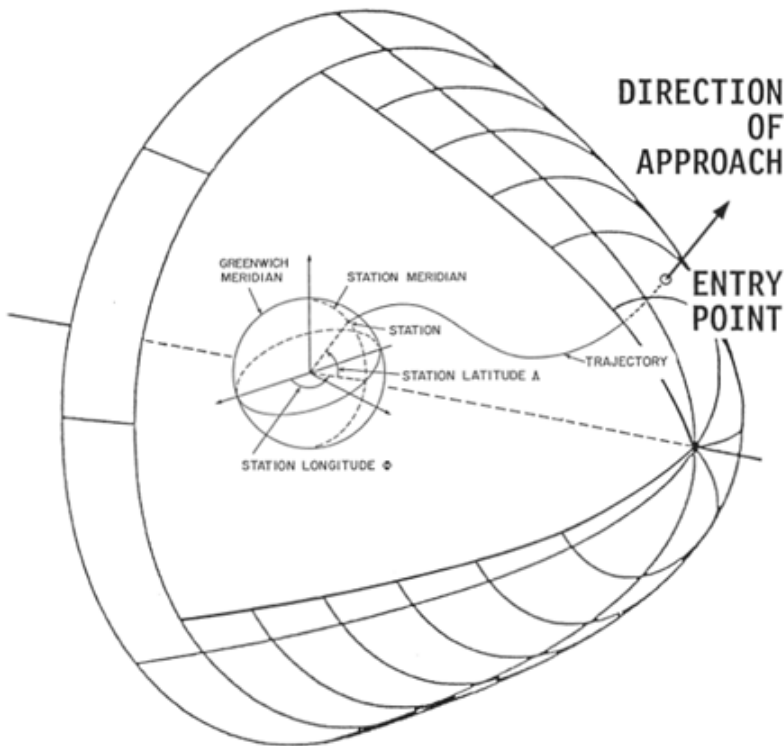
Red: strong correlation ($|R| \geq 0.7$). **Blue:** good correlation ($0.7 > |R| \geq 0.5$).

Green: weak correlation ($0.5 > |R| \geq 0.3$). **Black:** no correlation ($|R| < 0.3$).

SEP anisotropies

Trajectory analysis

Motivation



[Shea & Smart, ERP No 524, AFCRL-TR-75-0381, 1975]

- ❖ In order to measure SEP angular distributions (and investigate the degree of anisotropy), it is necessary to account for the effect of the geomagnetic field on particle propagation.
- Typically (NMs) one is interested in particle arrival "**asymptotic directions**", i.e. the directions of approach before they enter the magnetosphere.
- ✓ To determine asymptotic directions, particle trajectories are reconstructed in a model magnetosphere by means of **numerical integration methods** (Smart & Shea 2005).
- ★ The trajectory analysis also allows to evaluate geomagnetic cutoff rigidities and to separate protons of interplanetary (GCRs & SCRs) and atmospheric (trapped & albedo) origin.

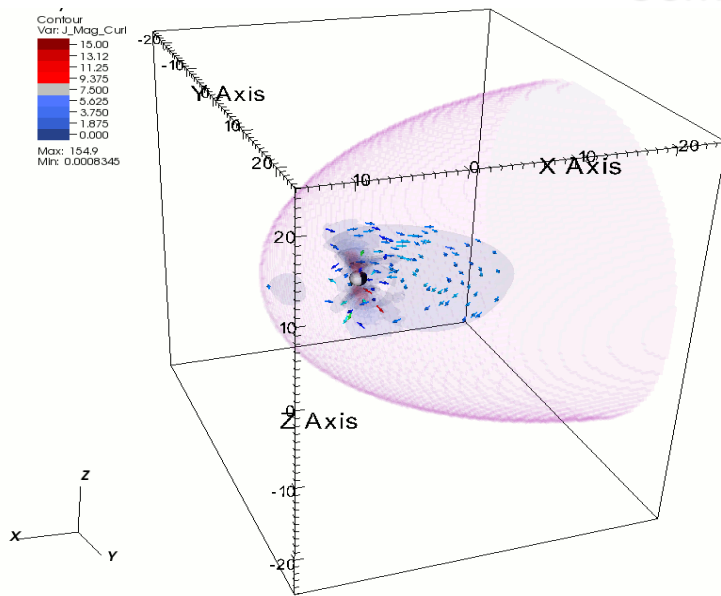
Trajectory analysis

Gemagnetic field models

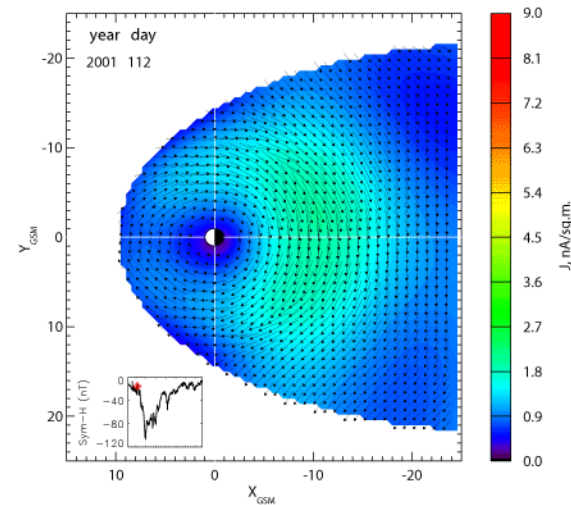
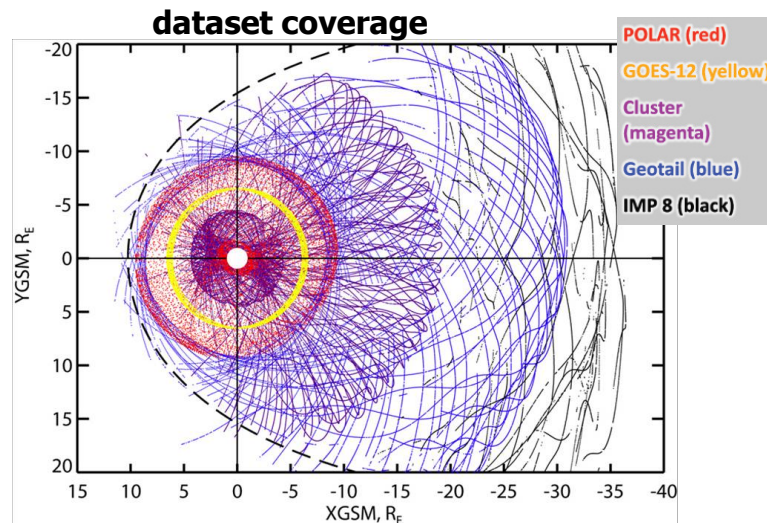
The Tsyganenko models are **semi-empirical** best-fit representations for the external magnetic field

The **TS07D** model (Tsyganenko & Sitnov 2007):

- ❖ Dynamical, high-resolution description:
 - large ($\sim 10^6$ points) dataset based on recent (1995-2005) spacecraft measurements (Cluster, Polar, Geotail, IMP-8, GOES 8-12);
- ❖ Coverage: $< 30-35 R_E$;
- ❖ **More flexible and strongly superior to all past empirical models in reconstructing distribution of storm-scale currents.**

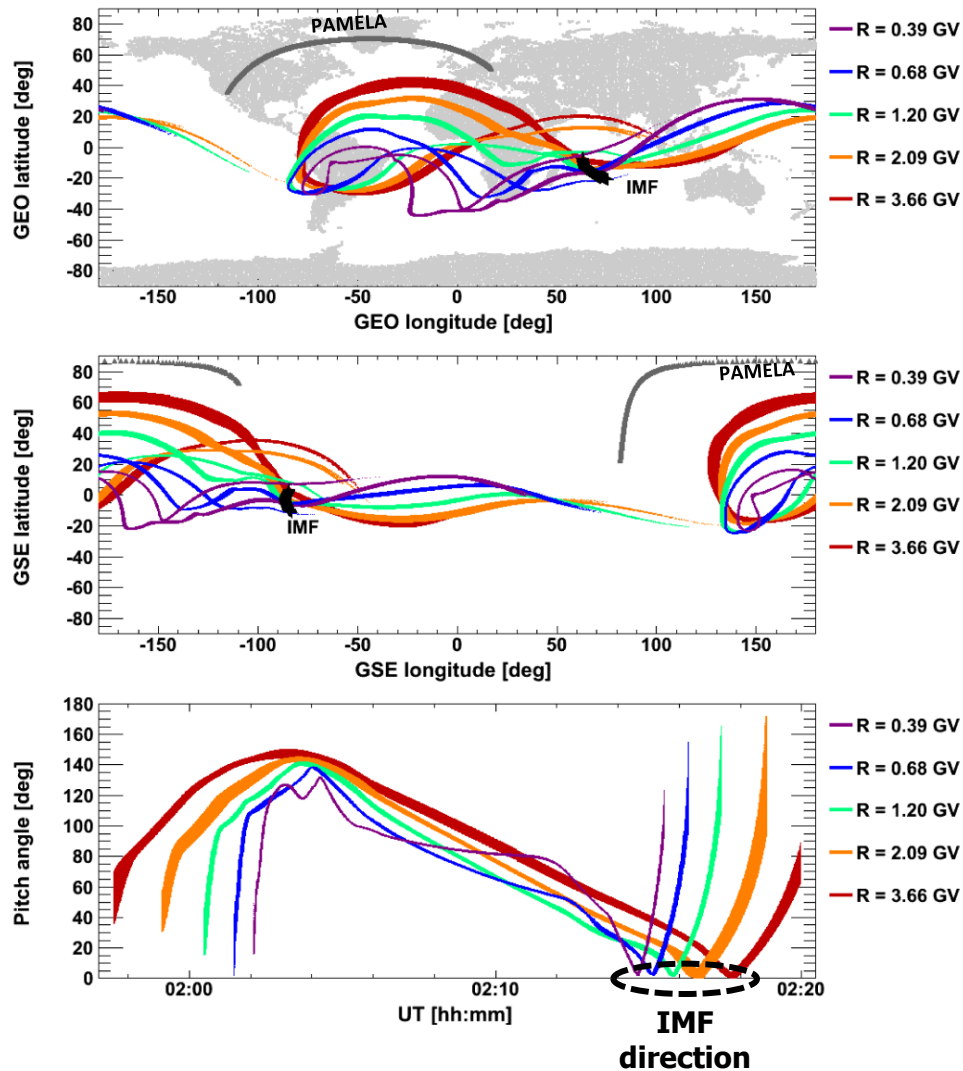


For more details: http://geomag_field.jhuapl.edu/model/



The 2012 May 17 event

Effective area calculation



- **Asymptotic cones of acceptance** evaluated for the first PAMELA polar pass (01:57÷02:20 UT) during the May 17, 2012 SEP event. Results for sample rigidity values are shown as a function of GEO (**top panel**) and GSE (**middle panel**) coordinates;

- The pitch-angle coverage as a function of the orbital position is displayed in the **bottom panel**.

- ❖ During the satellite polar pass the asymptotic cones move in a clockwise direction and a large pitch-angle interval is covered (0÷145 deg).

- ✓ In particular, PAMELA is looking at the IMF direction between 02:14 and 02:18 UT, depending on the proton rigidity.

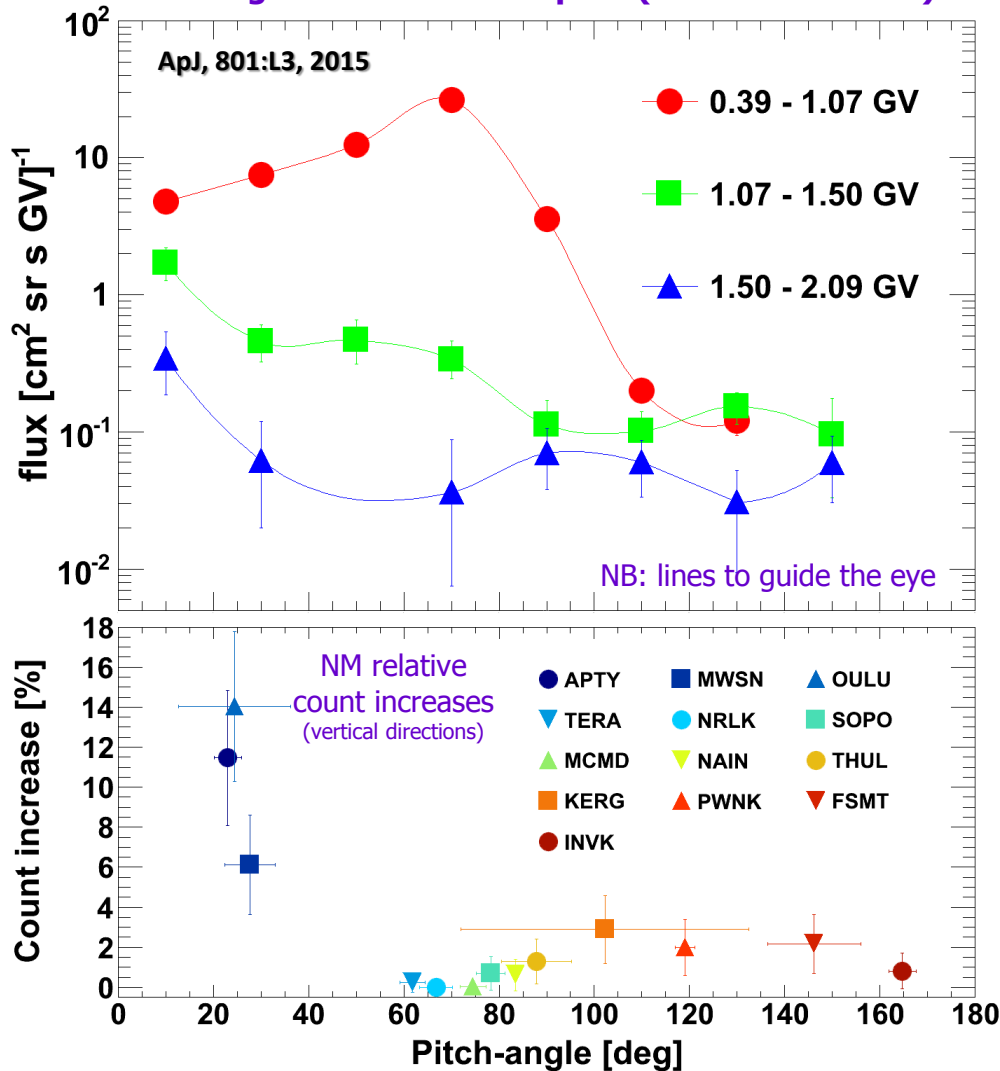
Fluxes are averaged over the polar pass (~22 min)

The 2012 May 17 event

Pitch-angle distribution

PAMELA vs NMs

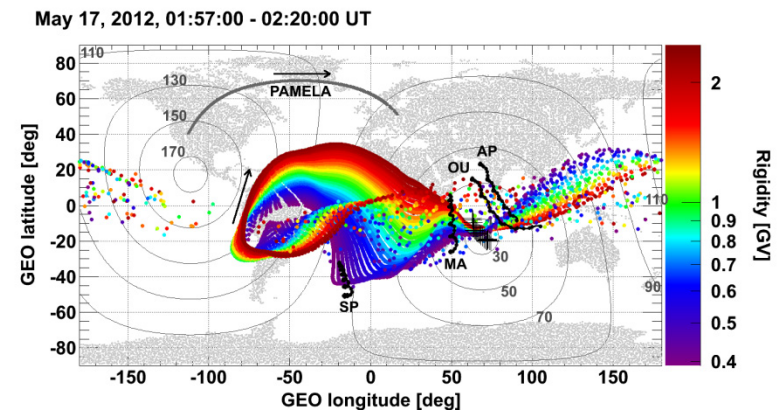
averaged over the solar pass (01:58 - 02:20 UT)



PAMELA observes two populations simultaneously with very different pitch angle distributions:

- a low-energy component (<1 GV)
 - confined to pitch angles <90°
 - and exhibiting significant scattering or redistribution;
- and a high-energy component (>1.5 GV)
 - beamed with pitch angles <30°,
 - consistent with NM observations.
- The component with intermediate energies (1 - 1.5 GV) suggests a transition between the low and high energies.

At rigidities >1 GV, corresponding to NM data, the particles are mostly field aligned.



Summary

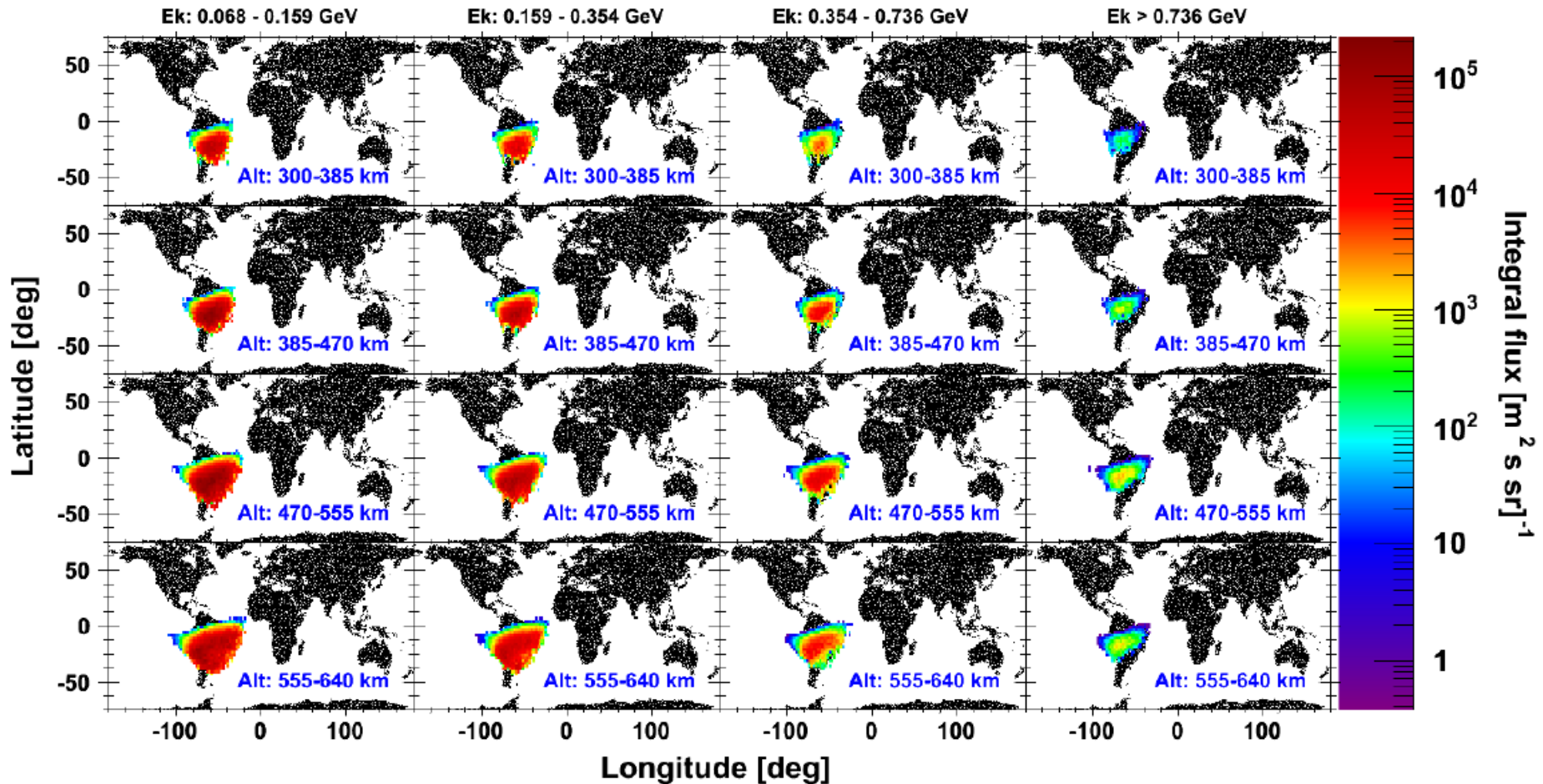
- PAMELA is providing comprehensive measurements of SEP events at high energies (>80 MeV)
 - 27 SEP events, including 2 GLE and 1 sub-GLE
 - spectra/fluences, angular distributions, composition
 - Data were compared with main flare/CME parameters, investigating possible correlations, including their dependency on energy

Spare slides

Geomagnetically trapped protons

Geographic Maps

columns: same energy bins
rows: same altitude bins

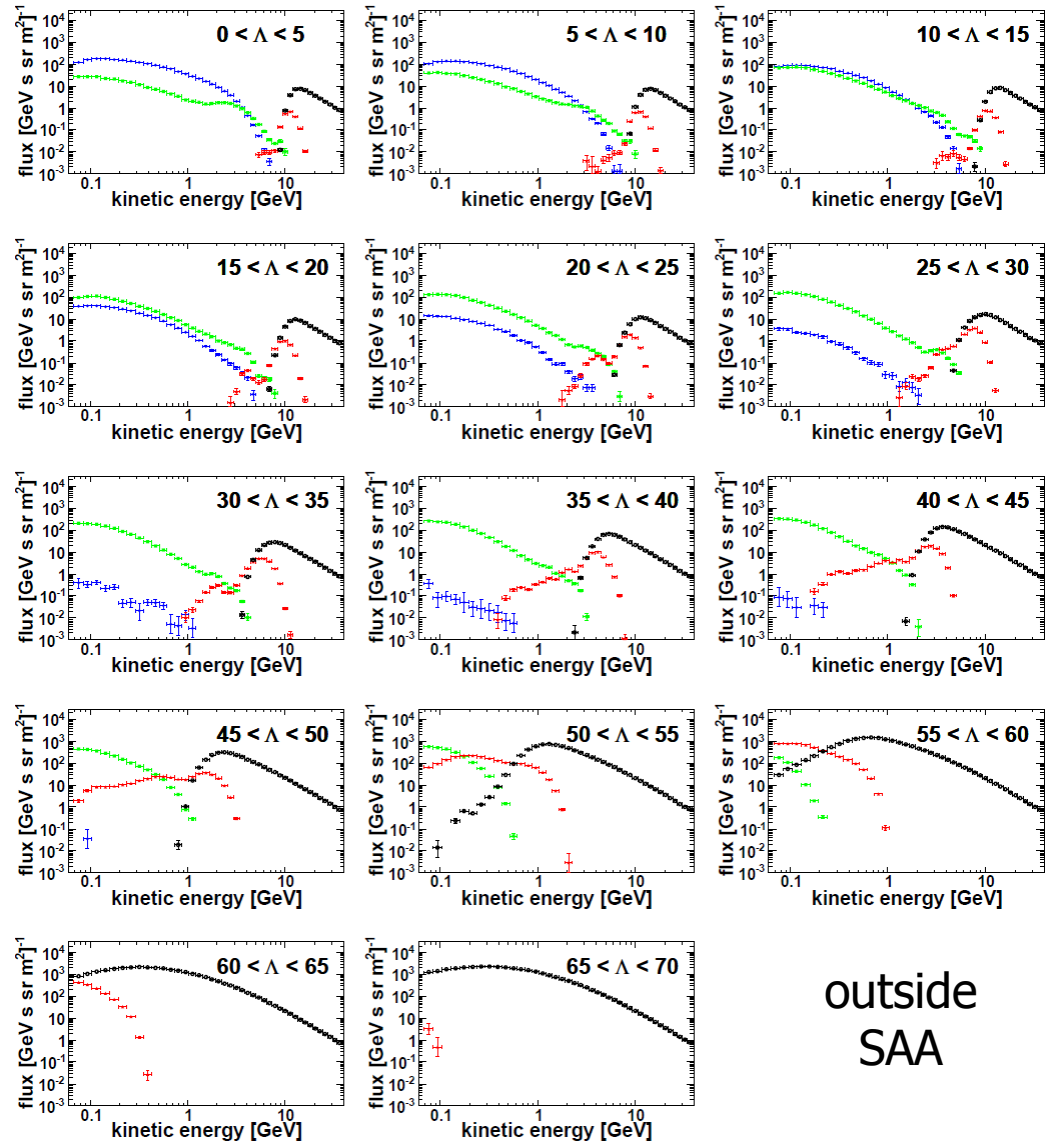


Stably-trapped integral flux ($m^{-2}s^{-1}sr^{-1}$) averaged over the pitch angle range covered by PAMELA, as a function of **geographic coordinates**, evaluated for different energy (columns) and guiding center altitude (rows) bins.

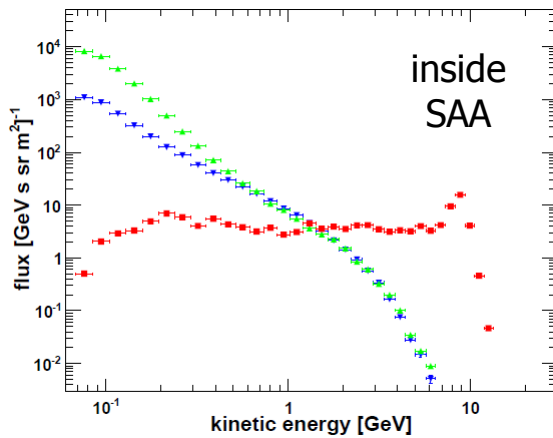
Albedo protons

Energy spectra vs latitude

Differential energy spectra outside the SAA region measured for different bins of magnetic latitude (see the labels).



Results for the different proton populations are shown: quasi-trapped (**blue**), precipitating (**green**), pseudo-trapped (**red**) and interplanetary (**black**).



Differential energy spectra in the **SAA** region ($B < 0.23$ G)

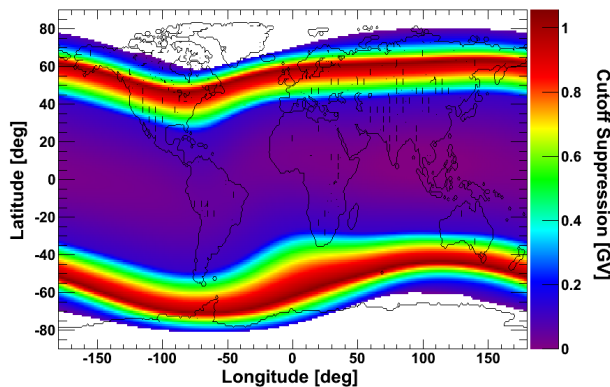
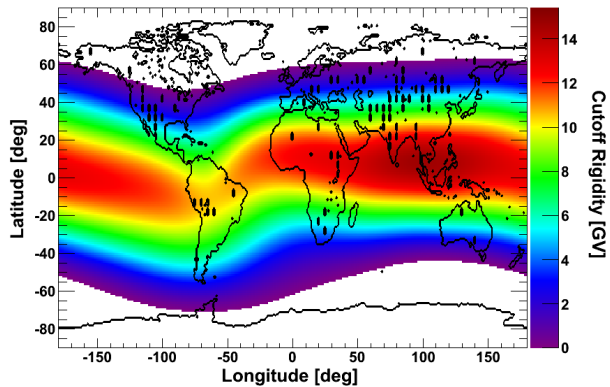
outside
SAA

Geomagnetic effects

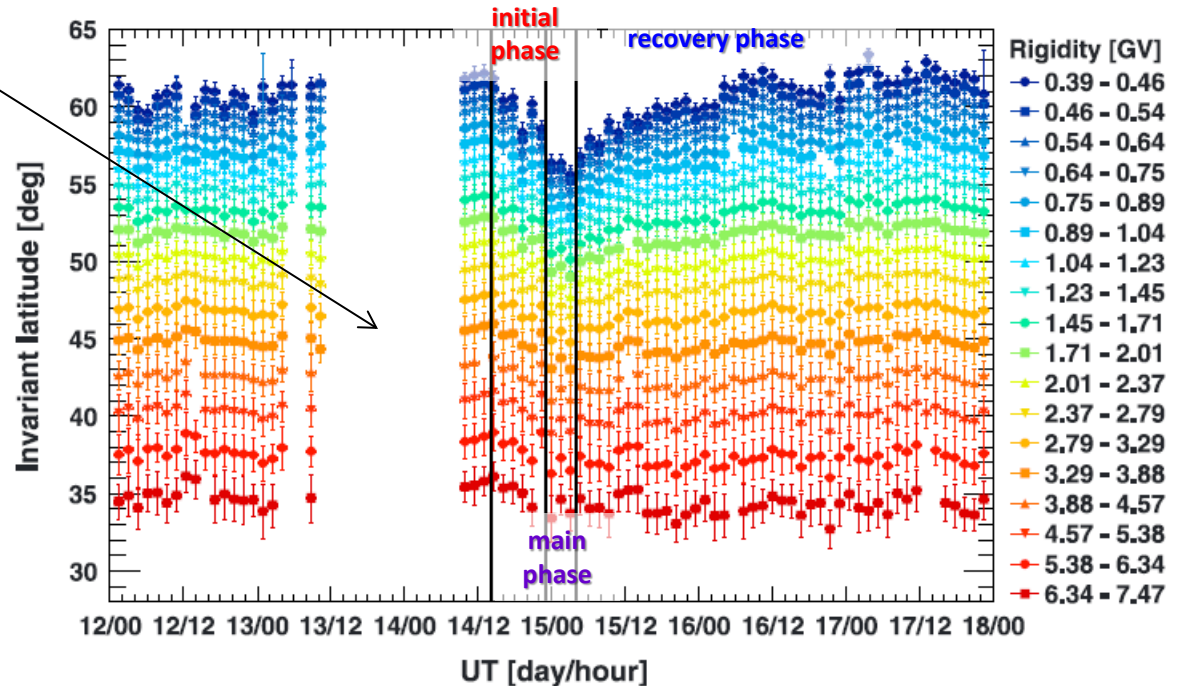
the 2006 Dec 14 magnetospheric storm

Data missing from 10:00 UT on Dec 13 until 09:14 UT on Dec 14 because of an onboard system reset of the satellite

Time profile of the geomagnetic cutoff latitudes measured by PAMELA for different rigidity bins



cutoff map at time of maximum suppression



The evolution of the magnetic storm followed the typical scenario in which the cutoff latitudes move equatorward as a consequence of a CME impact on the magnetosphere with an associated transition to southward IMF B_z .

Adriani et al., Space Weather, 14, 2006